Quality of sea-ice habitat traversed by Antarctic krill larvae influences recruitment

Supplementary Information

Devi Veytia[1*], Sophie Bestley[1,2], Klaus M. Meiners[2,3], So Kawaguchi[2,3], Eugene J. Murphy[4], Kazuya Kusahara[5], Stuart Corney[1,2]

1. Institute for Marine and Antarctic Studies, University of Tasmania, 20 Castray Esp., Hobart, Tasmania 7000, Australia
2. Australian Antarctic Program Partnership, Institute for Marine and Antarctic Studies, University of Tasmania, Hobart, Tasmania 7004, Australia
3. Australian Antarctic Division, Department of Agriculture, Water and the Environment, 203 Channel Highway, Kingston, Tasmania 7050, Australia
4. British Antarctic Survey, High Cross, Madingley Road, Cambridge CB3 0ET, UK
5. Japan Agency for Marine Earth Science and Technology (JAMSTEC), Yokohama, Kanagawa 236-0001, Japan

* corresponding author. E: Devi.Veytia@utas.edu.au

Appendix A. Data processing: Nominalizing recruit density

As a response variable, regional indices of recruitment present statistical challenges due to their high natural variability, sparse sampling coverage, and spatial heterogeneity. As noted in [1], there was a high occurrence of sampling seasons with a recruit density of zero. This not only introduces statistical complications such as zero-inflation and over-dispersion, but also raises the important issue of sampling error and whether the observed years of zero recruitment are an accurate representation of the population. Acknowledging that there is likely higher sampling error surrounding recruit density as a continuous variable, we chose to take a more robust approach by nominalizing recruit density. This allows us to compare differences in along-trajectory habitat between high and low recruitment years

We used hierarchal clustering to classify values into ordinal categories representing high, moderate and low recruitment years. For each region, a Euclidean distance matrix was computed on the log-transformed recruit density (to avoid infinite log values, a small value of $1x10^{-5}$ was added to zero values before logging) for all the recruit density values. An average linkage sorting strategy was used to determine the hierarchal clusters using the *hclust* function[2]. These hierarchal clusters were then split into three groups using *cutree*[2].

Appendix B. Sensitivity analyses

To test the robustness of our results to our analysis, we conducted a sensitivity analysis for each of our assumptions throughout our analysis. Here we describe the methods and results pertaining to each of the sensitivity analyses.

B.1 Nominalizing recruit density

To nominalize recruit density, hierarchal clustering with an average linkage sorting strategy was used in the main analysis, as this was the most moderate sorting strategy. We also trialled single (nearest neighbour) and complete (furthest neighbour) linkage and compared these results to those obtained from average linkage. These hierarchal clusters were then split into three groups using *cutree*[2]. The groupings were relatively robust to changes in sorting strategy (Supplementary Fig. B.1) and therefore the average method was used in the study.

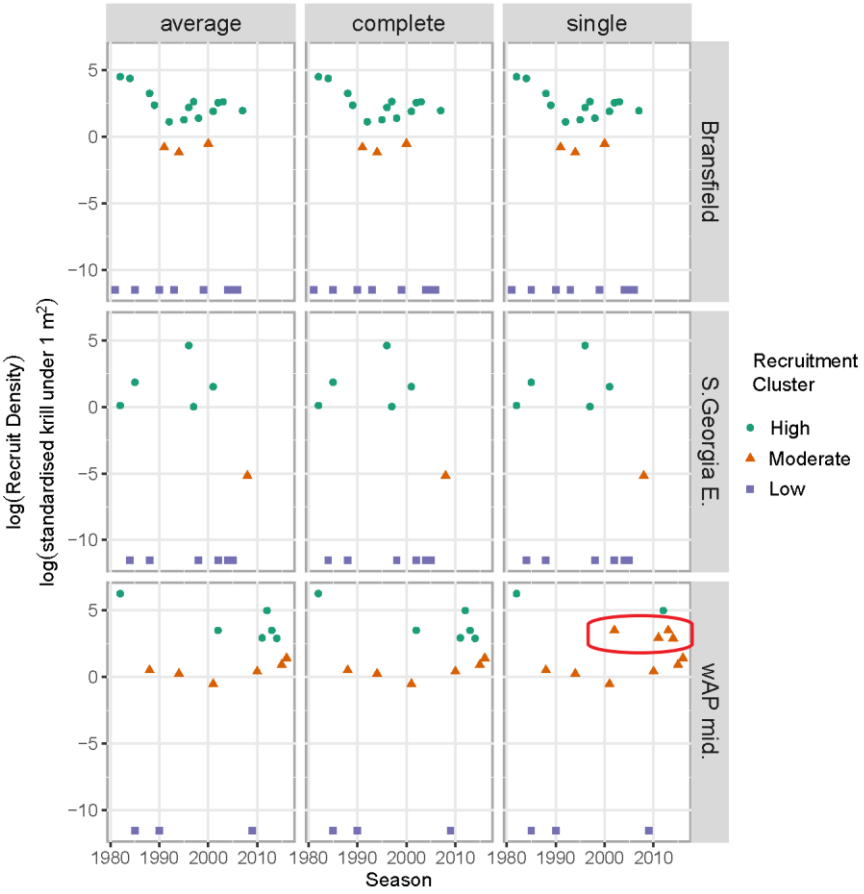

Figure B.1. Sensitivity of nominalization of recruit density to sorting strategy. Here we compare three sorting strategies for determining hierarchal clusters: average, single (nearest neighbour) and complete (furthest neighbour). Average linkage was used in the analysis, but the results were robust to changes in sorting strategy – the only difference being in the classification of high recruitment years from 2000-2016 in the wAP mid (see red oval).

B.2 Simulating particle back-trajectories

In the main analysis, monthly-averaged velocity fields for both sea ice and ocean surface currents were used to calculate the Lagrangian back-trajectories. However, as daily model output for these velocities were available, we examined the differences arising from using higher resolution daily output compared to the monthly output for three years representing high, moderate and low recruitment (1982, 1992 and 2006 respectively), calculated from a recruit density time series pooled across the southwest Atlantic[3].

We found that the differences between the binned counts of particle trajectories calculated from daily vs monthly velocities were negligible (Fig B.2). Not including cells that had infinite differences (which occurred when particles passed through a cell when calculated with monthly velocities but not with daily, totalling 47/993 cells), 95% of cells had an absolute difference < 1.78x the daily count. These larger differences often occurred at the ends of trajectories. However, the majority (75%) of absolute differences were a fraction of the daily count. We concluded that trajectories calculated from monthly velocities were sufficiently accurate to give us an estimate of particle transport at these spatial scales.

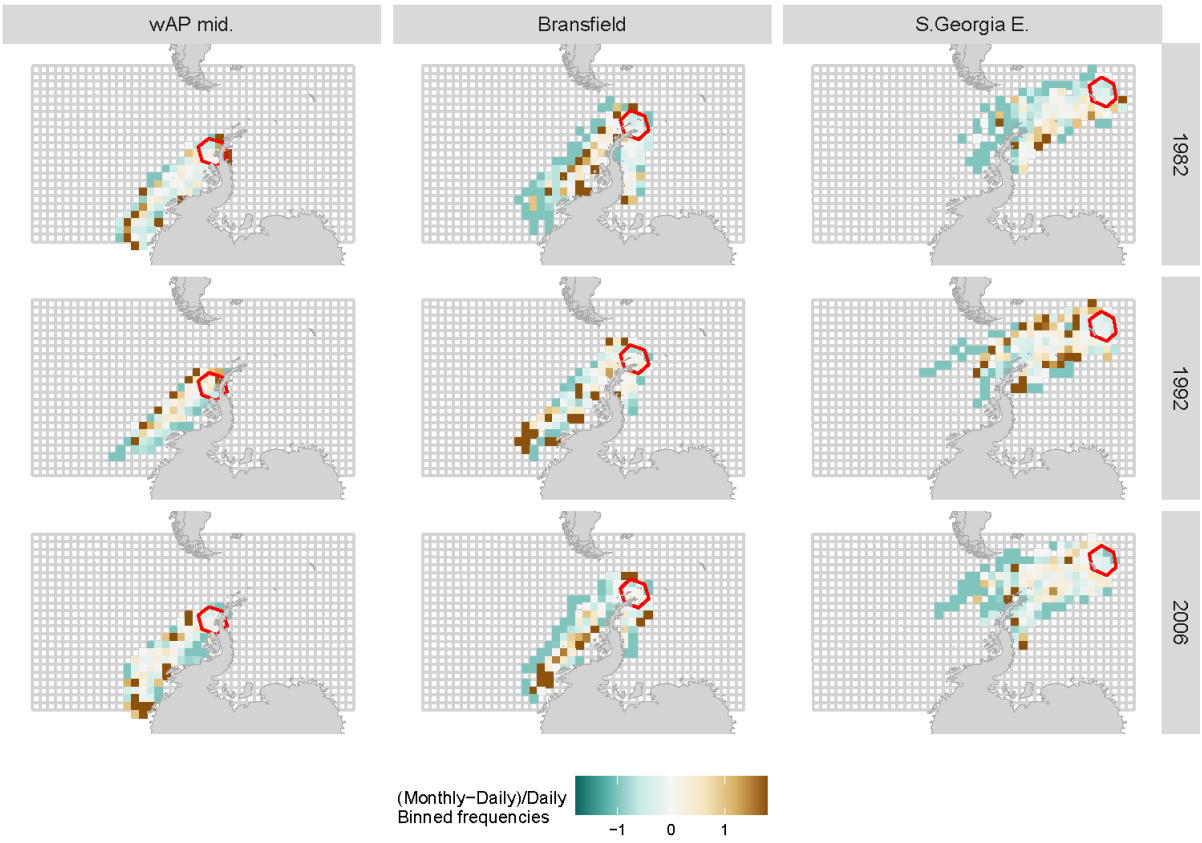

Figure B.2. Proportional differences in binned counts of particle trajectories calculated from monthly vs daily velocities. For each year: 1982, 1992 and 2006, Lagrangian back trajectories were calculated from daily and monthly-averaged velocity fields from Julian day 330 to 90. Particle positions were recorded every 10 days and binned to an equal-area grid. This figure displays the difference in binned counts of these particle locations between those calculated from monthly vs daily velocities, as a proportion of the binned counts calculated from the daily velocities. Therefore, a value of 1 would indicate a difference equal in magnitude to the number of particles in that cell from the daily velocity dataset.

Our choice to simulate larval advection with 12 h of being advected with sea ice and 12 h with ocean surface currents was informed by observational evidence[4]. However, to understand the influence of this assumption, we chose to explore how varying associations with sea ice and ocean advection would impact our results. To achieve this, for an average recruitment year (1992) we calculated Lagrangian back-trajectories for scenarios where particles were advected 100% of the day with sea ice, to 0 % (all ocean) in intervals of 25%. Where sea ice was absent ocean velocities were used. Particle locations were updated every 6 h. For example, for the 25% scenario, the particle was advected with sea ice for one timestep, and with ocean surface currents for the remaining three timesteps.

Our results revealed that adding sea ice transport influenced the spatial distribution of particles, particularly in aiding particle transport from South Georgia through the Scotia Sea (Supplementary Fig. B.3). There was little difference between 50-75% sea ice transport. Therefore, our transport results are not highly sensitive to varying associations of transport with sea ice, so long as more than a 25% association with sea ice is assumed.

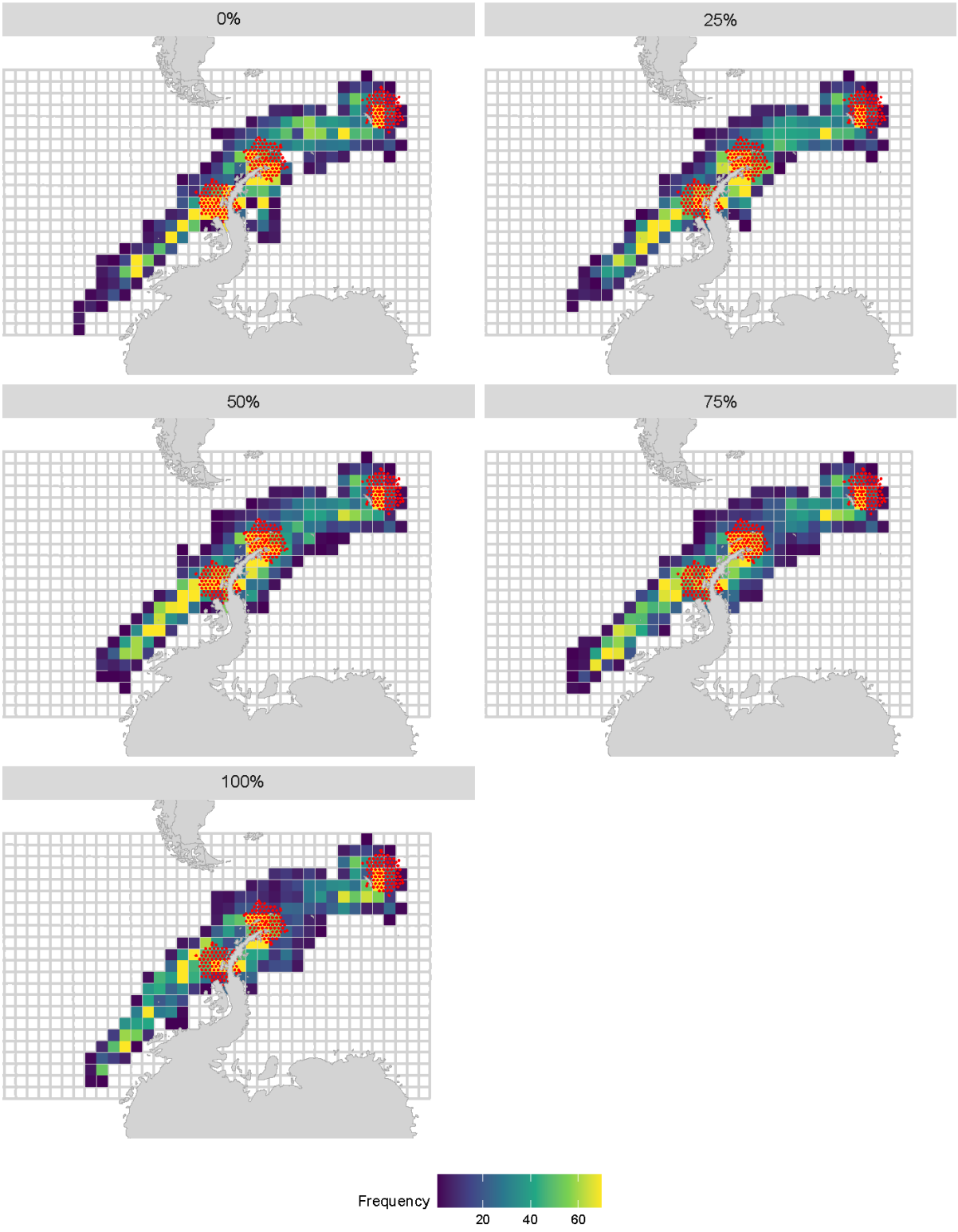

Figure B.3. Binned frequencies of Lagrangian back trajectories resulting from varying associations with sea ice transport. Particles were seeded on Julian day 330 within the three recruitment regions (seed locations indicated by red dots), and back-trajectories were calculated to Julian day 90. Particle positions were recorded every 10 days and binned to an equal-area grid. Panel titles (0, 0.25, 0.5, 0.75, 1) reflect the percentage of each day that a particle was advected with sea ice as opposed to ocean surface velocities. Therefore panel “0%” is purely ocean advection, whereas panel “100%” is advected with sea ice velocities, with ocean advection only used when sea ice was absent.

B.3 Quantifying along-trajectory habitat presence and continuity

As described in the manuscript, a series of continuity rules (Fig C.2) were applied to our habitat presence filter assess habitat continuity. These included:

1. The day that the continuity rules begin (Julian day 182);
2. A starvation threshold of 30 days; and
3. The day after which a particle can emerge from the sea ice and survive (see Appendix C).

To examine the influence of these assumptions on our results, we conducted a sensitivity analysis, where the values of one continuity rule were varied while the others were held constant at their chosen values. Specifically, rule 1 was varied between Julian day 92-272 in increments of 15 days, rule 2 between 10-50 days in increments of 10 days, and rule 3 between Julian day 130-320 in increments of 10 days. At each iteration, the % of trajectory continuity was calculated as a response metric for each recruitment region and compared across high and low recruitment years.

Overall, we found that the proportion of trajectories that experienced continuity responded linearly to changes in continuity rules, and crucially that the difference between high and low recruitment years remained consistent (Supplementary Fig. B.4). As our analysis focuses on contrasting the differences in environment between high and low years, we deemed that our results are robust to changes in continuity rule assumptions.

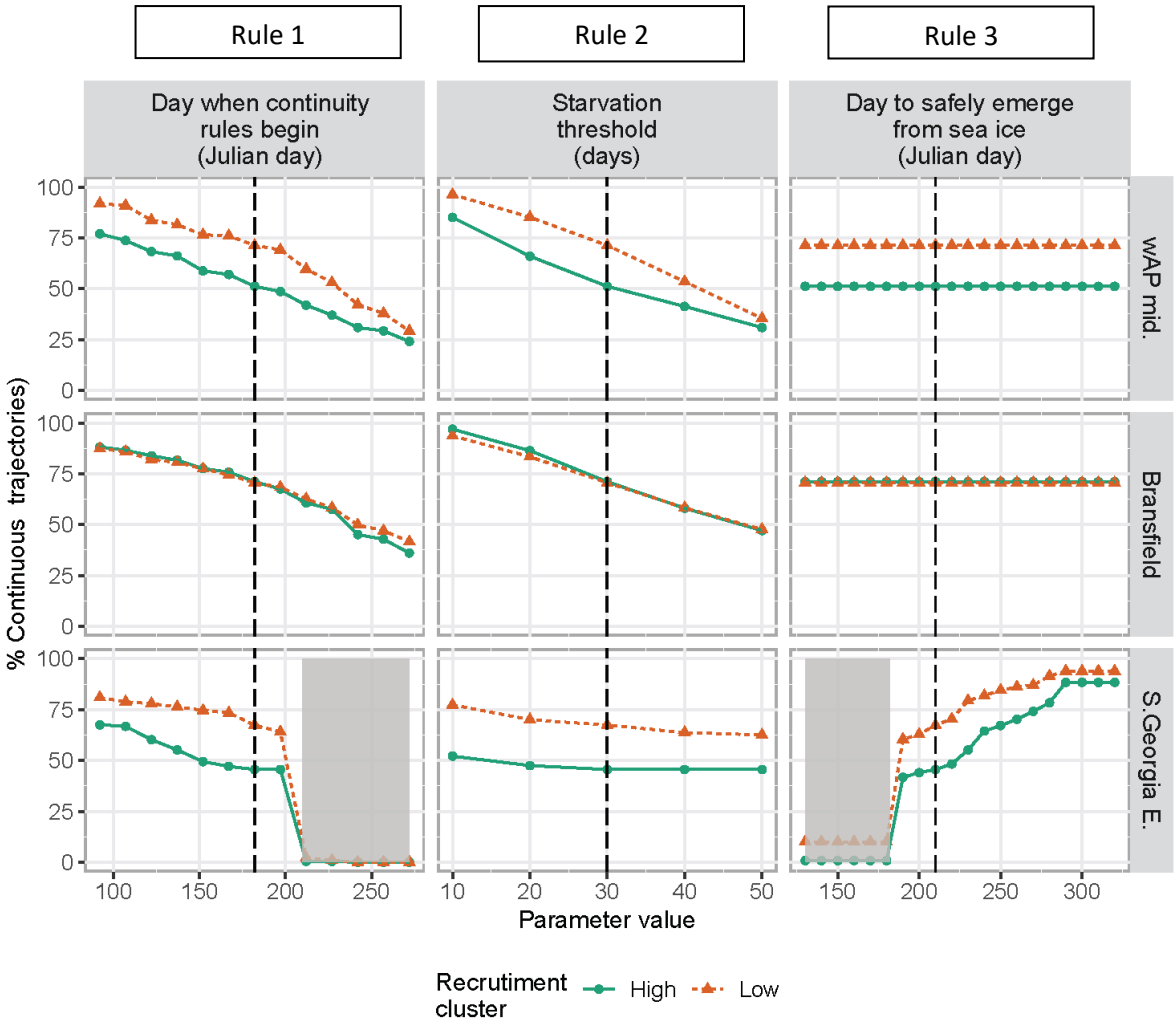

Figure B.4. Sensitivity of percent continuity (across all trajectories within a region and recruitment classification) in response to varying continuity rules. The black vertical dashed line indicates the value used for that rule in this analysis. Being that as one rule is varied the other rules are held at the values indicated by the black vertical lines, in the bottom row for S. Georgia E., a grey box indicates when another continuity rule takes over. For example, in the bottom left panel, continuity goes to zero after Julian day 210, as this is when rule 3 takes over and a particle is considered safe. If the start of the continuity rules occurs after this date, a particle is safe for the entirety of the simulation and not continuity occurs. Likewise, the grey box in the bottom right panel indicated the start of rule 1.

Appendix C. Continuity rules

Due to the geographical distance between South Georgia and the seasonal sea ice zone, it was likely that larvae destined for South Georgia would have different life histories and food sources than those along the wAP or Bransfield Strait. While our second hypothesis (Analysis step 2) speculates that increased time outside the sea ice would result in starvation, the oceanic waters en-route to South Georgia are at a lower latitude with increased light availability and thus pelagic phytoplankton growth may sustain larvae outside the sea ice.

To verify this, we used satellite ocean colour data to estimate average pelagic food availability. These comprised chlorophyll-a estimates from [5] that improved SeaWiFS ocean colour data for the Southern Ocean. These data were retrieved in daily timesteps from April 1 to November 30 from 1997 to 2010 using the *raadtools* package[6]. The original data had a very fine resolution of $<0.1^{o}$. To avoid aliasing when averaging over the sparse winter coverage, we binned these data to a courser 0.5^{o} resolution.

Examining satellite-derived chlorophyll-a concentrations in the surrounding waters as a proxy for pelagic food availability, we concluded that on average, particles encounter highly productive waters at day 270 (Supplementary Fig. C.1). It would be reasonable to assume that a larvae would have adequate access to food in this environment, which would justify pushing the end of starvation threshold window back from day 330 to day 270. Furthermore, a laboratory experiment has quantified larval growth over 60 days of starvation[7]. This indicates that adjusting the length of our starvation threshold window from 30 to 60 days is reasonable. This evidence allows us to derive a feasible continuity rule 3. This continuity rule allows particles destined for S. Georgia E. to emerge from the sea ice on or after Julian day 210, after which a larva can be assumed to have adequate continuous habitat to reach the end of the simulation.

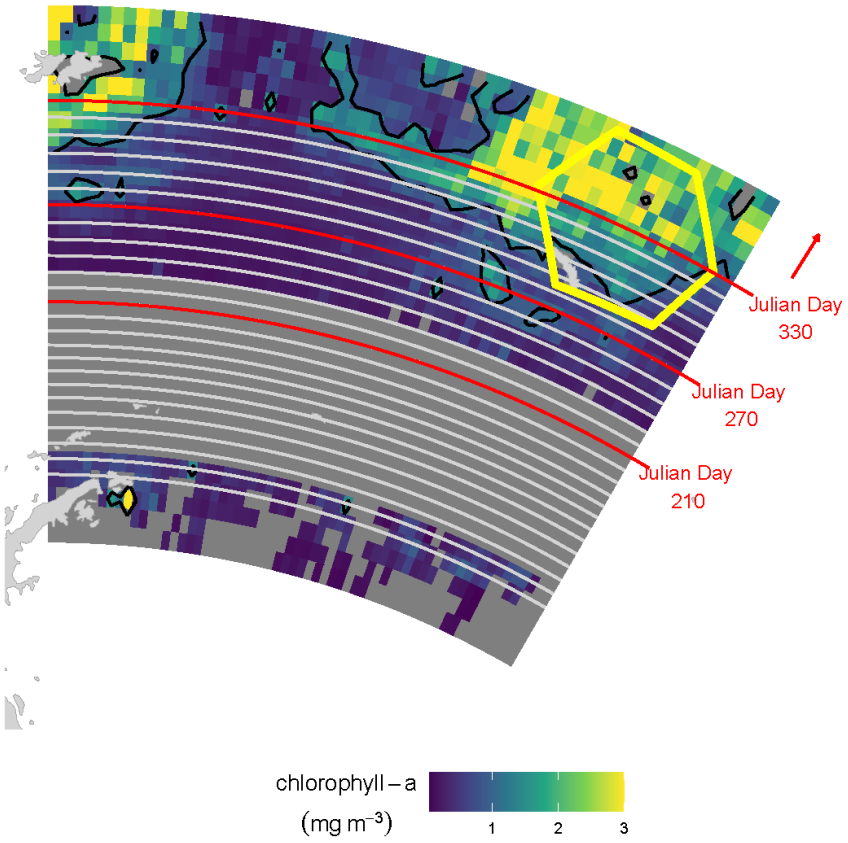

Figure C.1. Average chlorophyll-a concentration along an average trajectory to S. Georgia E. over the years 1997-2010. All trajectories going to S. Georgia E. (indicated by yellow hexagon) were averaged into one trajectory, yielding particle locations at 10-day intervals. Swaths of the corrected estimate of SeaWiFS chlorophyll-a data[5] were then averaged for each 10-day period (indicated by white latitudinal lines) and are shown by the colour bar (grey = "NA"). For example, cells between the bottom line (Julian day 90) and the next line up (Julian day 100) reflect an average of all daily chlorophyll-a data collected between Julian days 90 and 100 over the years 1997-2010. Black contours delineate high chlorophyll-a concentrations greater or equal to 1 mg m^{-3}. The top red latitudinal line indicates the particle position at the end of the simulation (Julian day 330). Moving southwards down the figure, the next red line indicates the particle position at Julian day 270, where high levels of pelagic chlorophyll-a concentration begin to be encountered. The southern-most red line at Julian day 210 indicates the start of rule 3, when a particle can emerge from the sea ice and is assumed to survive to the end of the simulation.

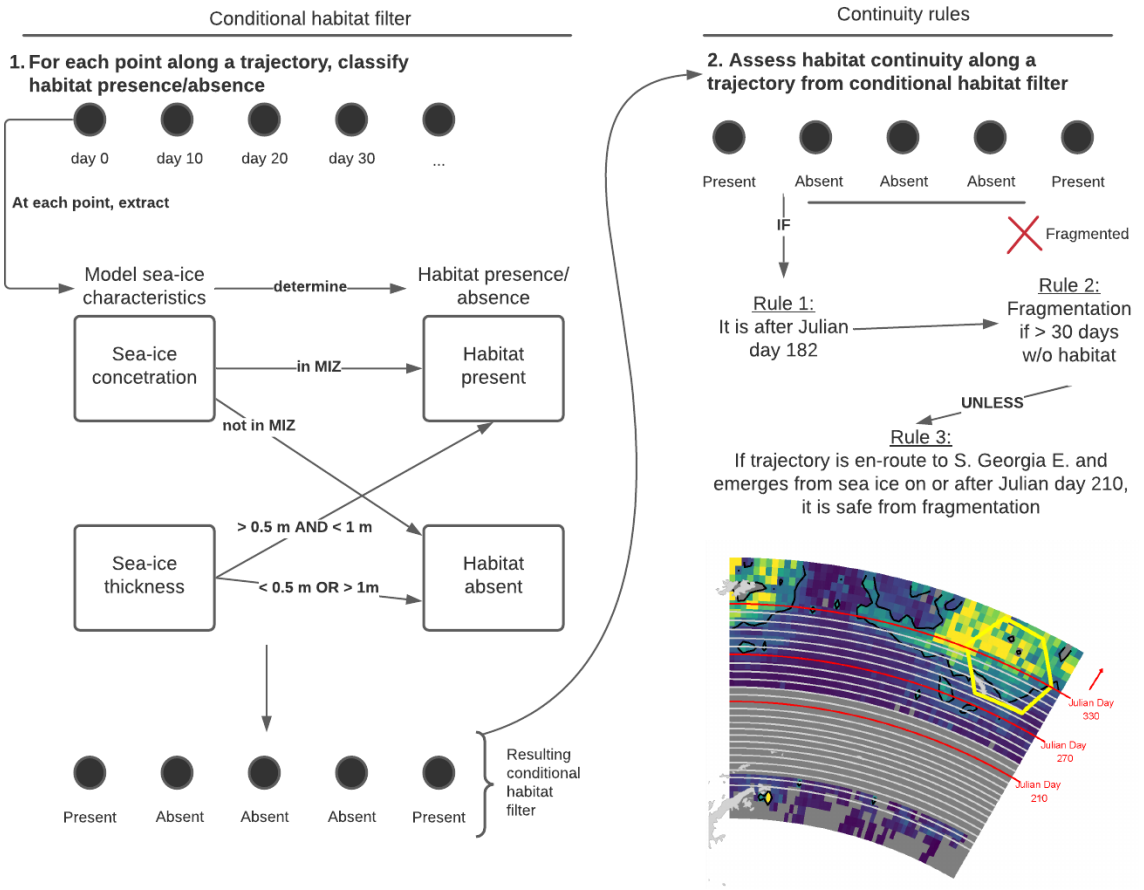

Figure C.2. Conceptual diagram describing habitat presence and continuity rules. Using the conditional habitat filter as an input, a set of three continuity rules were applied to determine if a trajectory possessed sufficient habitat continuity to support a larva's survival. If the conditions were not met, the trajectory was determined to be fragmented.

Appendix D. Supplementary results

Figures

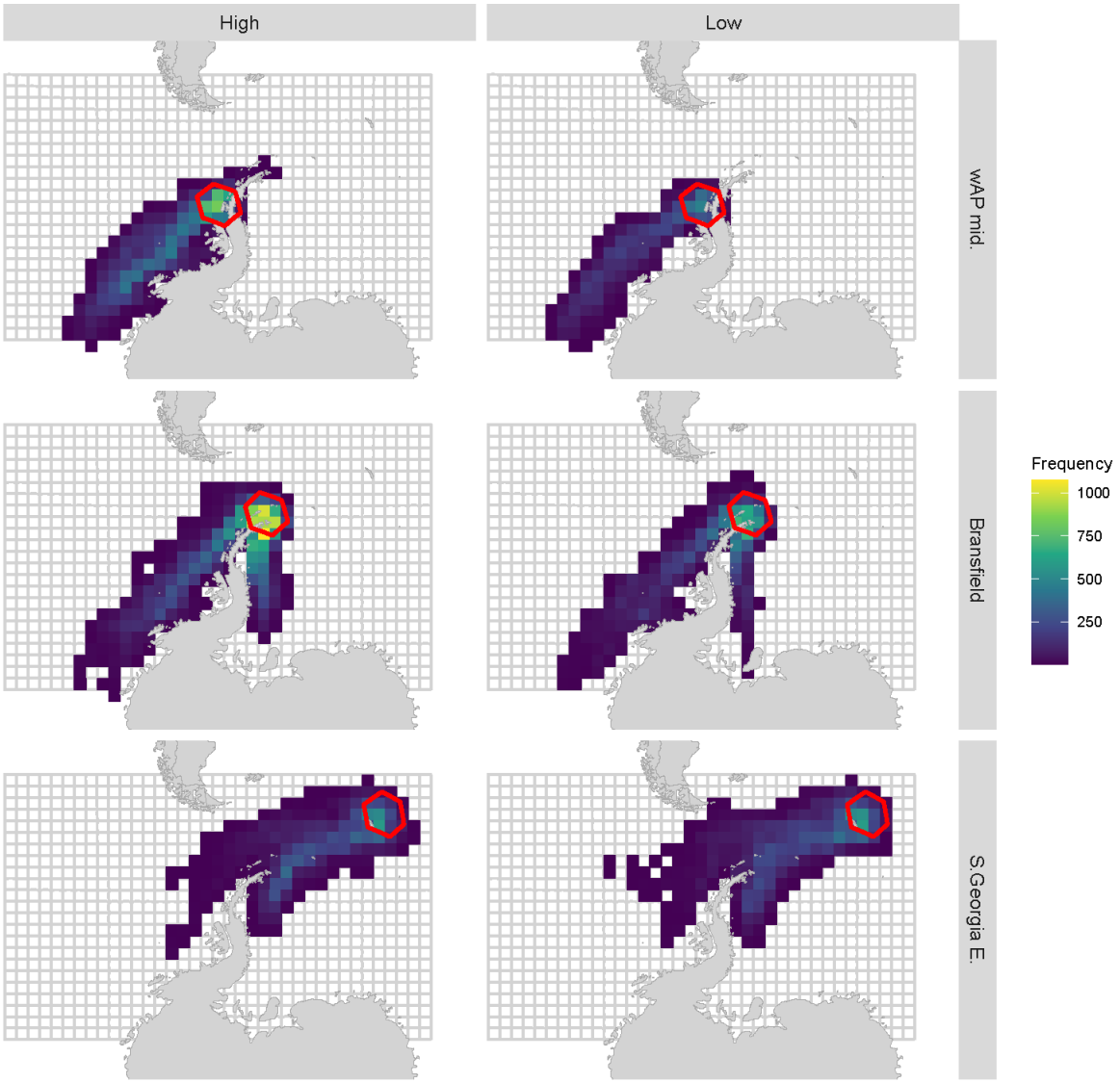

Figure D.1. Spatially binned particle locations over entire simulation. For all years classified as high or low recruitment, all particle locations (*i.e.* at 10-day intervals) were binned to an equal-area 150 km by 150 km grid. The counts of points occurring in each grid cell are represented by the colour ramp. Red hexagons indicate the recruitment region where the particles were seeded.

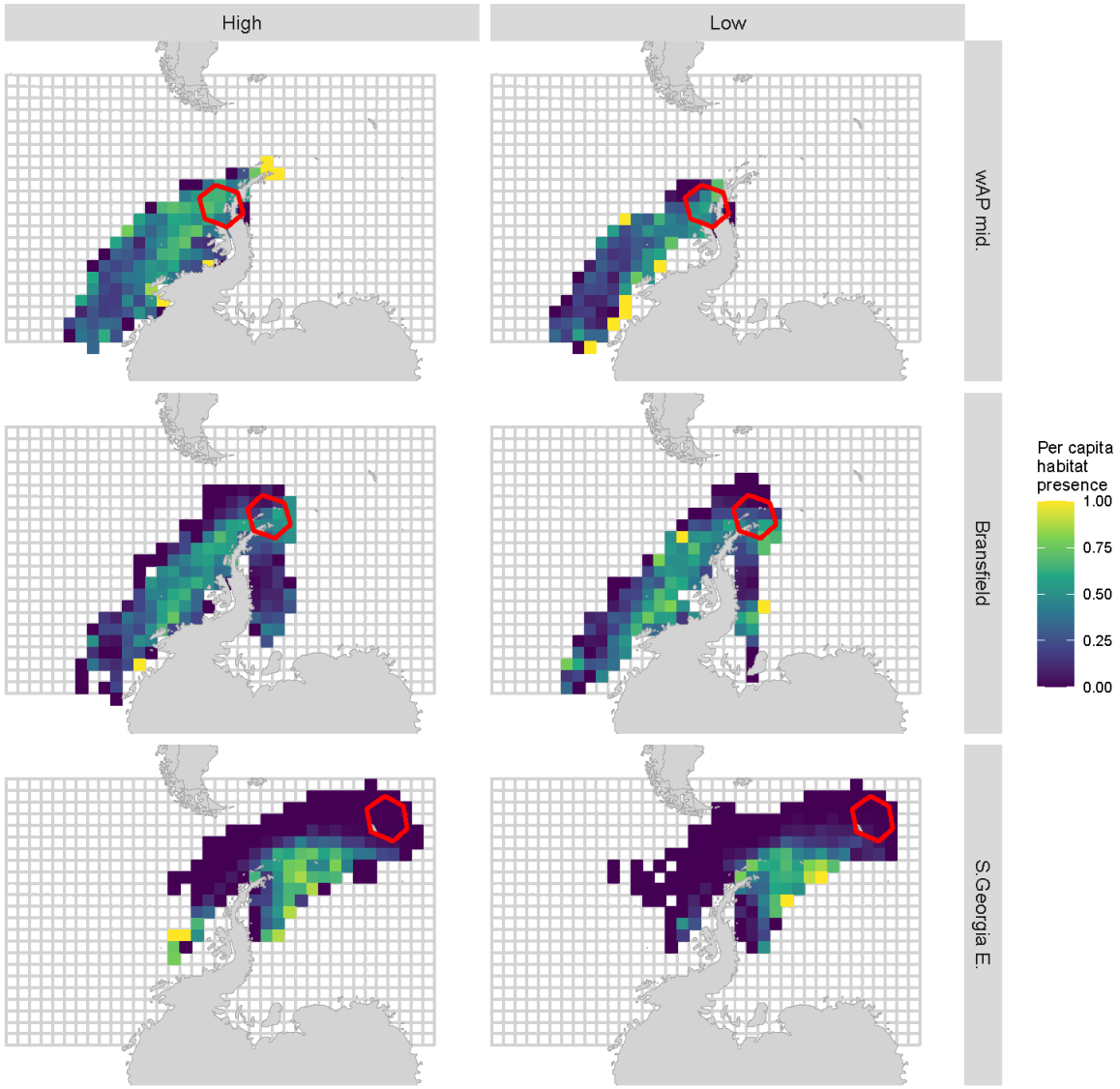

Figure D.2. Probability of encountering habitat. For each grid cell, the colour displays the number of times habitat was encountered in that cell, divided by the number of particles that have passed through that cell.

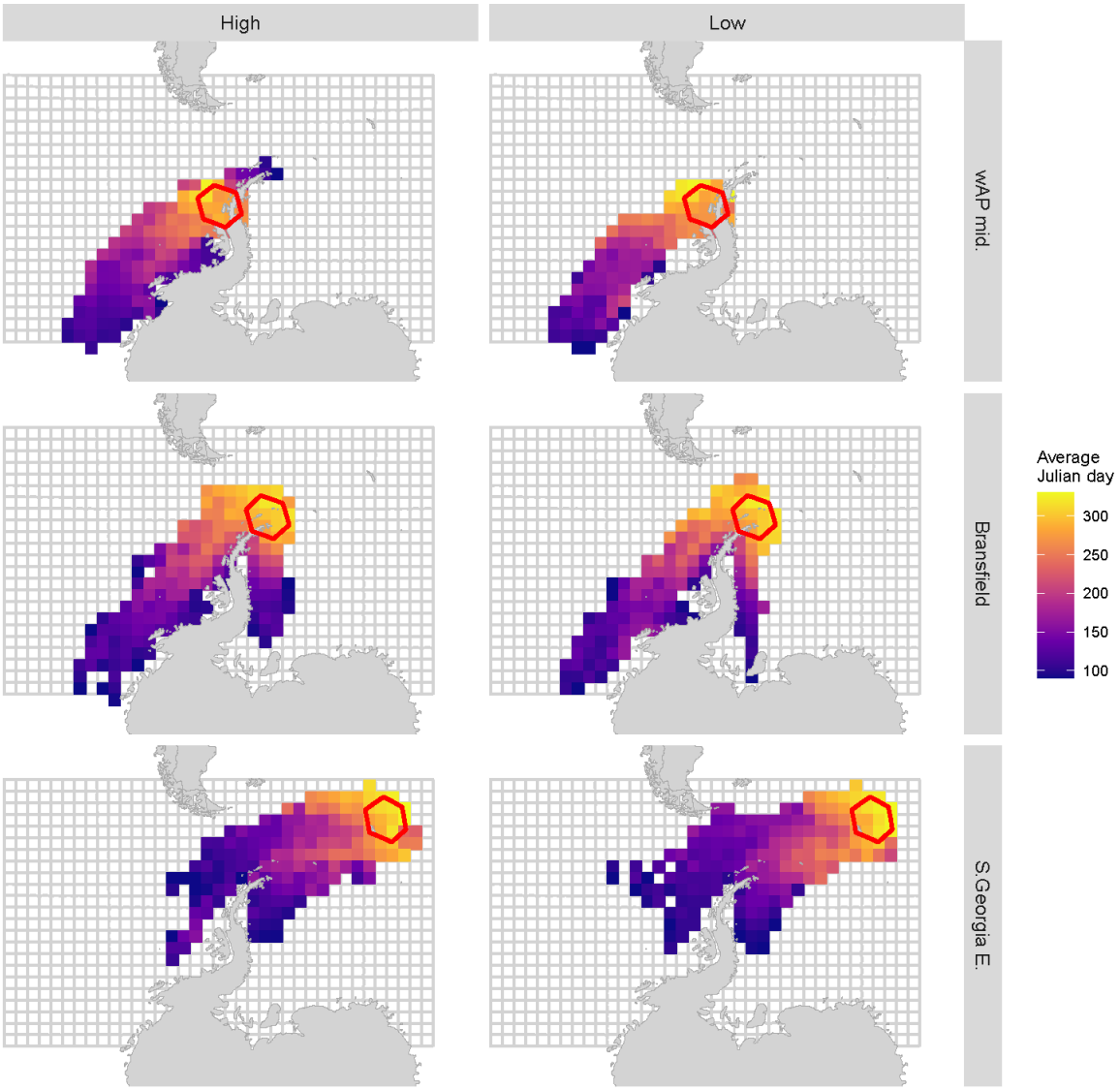

Figure D.3. The average timing of particle transport. The colour bar displays the average Julian day that particles passed through each grid cell, for each region and recruitment classification.

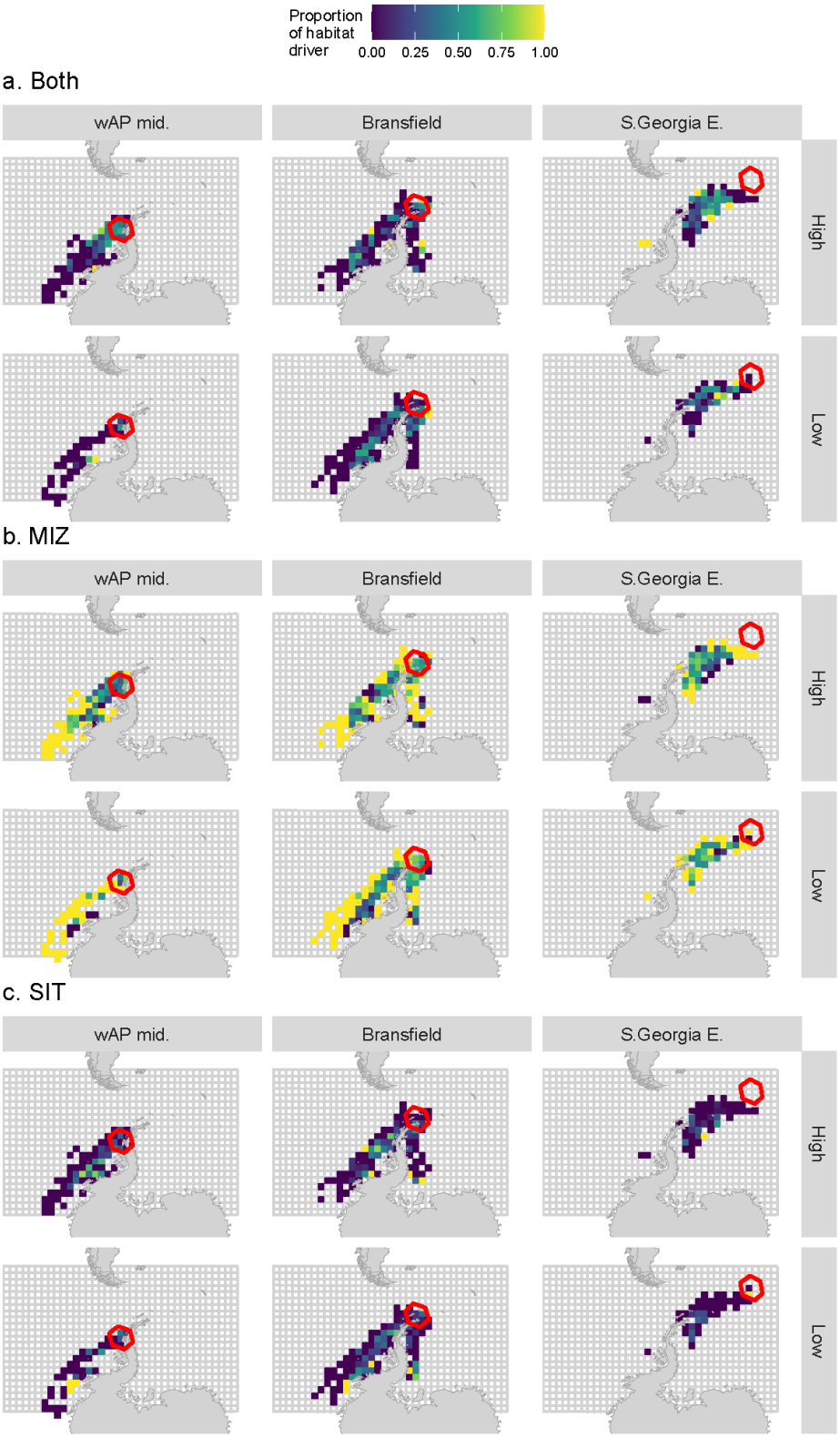

Figure D.4. The relative contribution of drivers of habitat presence: **a)** both presence of MIZ and optimal SIT between 0.5 m and 1 m; **b)** just the presence of the MIZ; or **c)** just the presence of optimal SIT between 0.5 m and 1 m. The proportional contribution of these three drivers are conditional on habitat presence (Supplementary Fig. D.2). Thus, of the number of times habitat was present within a given cell, this figure displays the proportion of those occurrences that are attributed to the three different drivers.

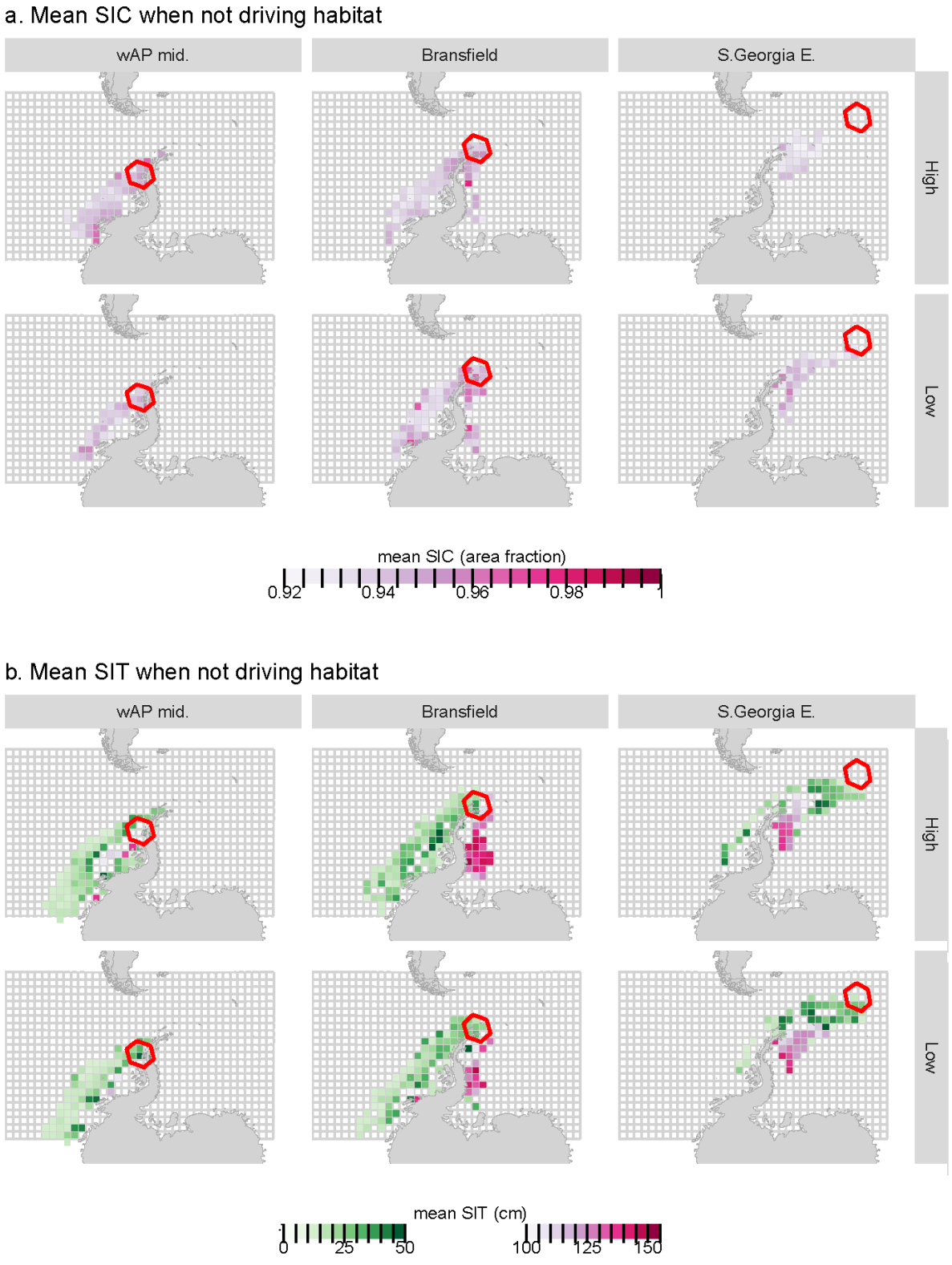

Figure D.5. The mean value of **a)** sea-ice concentration (SIC) and **b)** sea-ice thickness (SIT) when not driving habitat presence (Supplementary Fig.D.1).

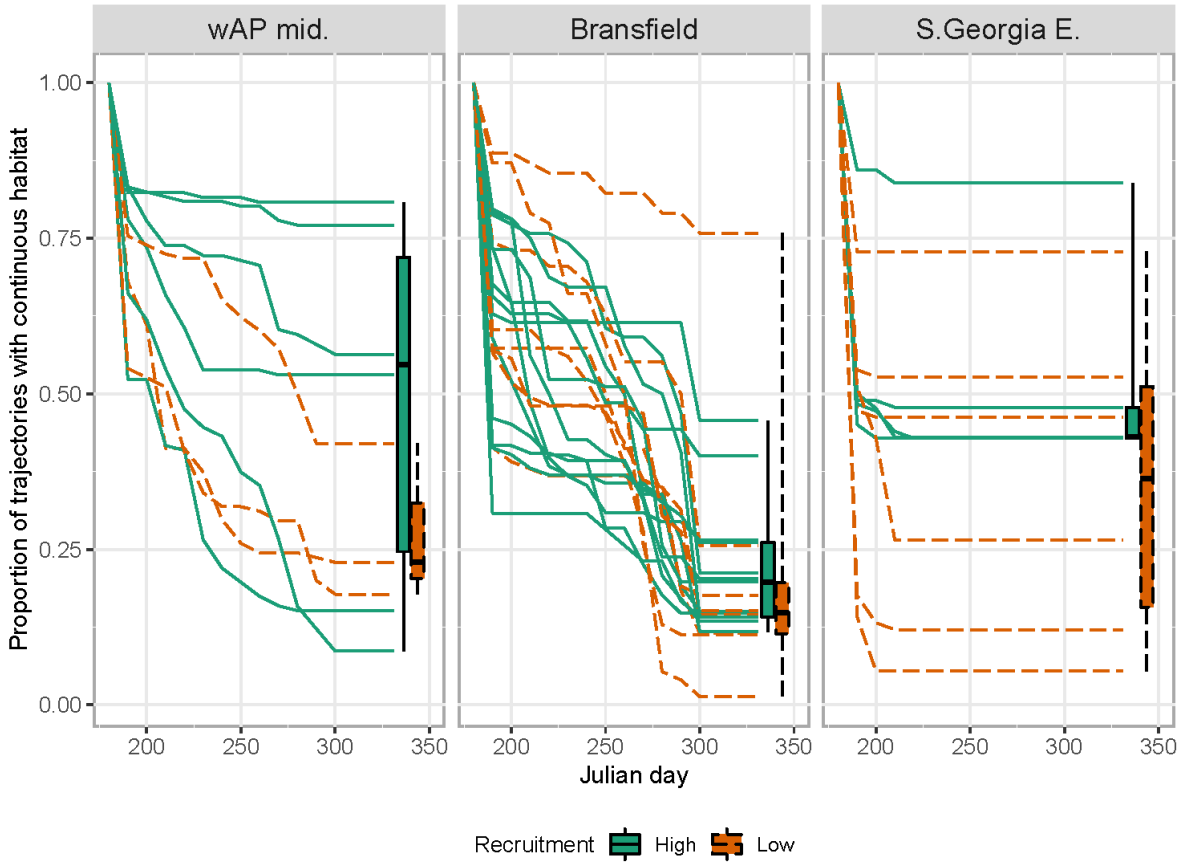

Figure D.6. The overwinter progression of the proportion of trajectories with continuous habitat as determined by the continuity rules (Appendix B) across high and low recruitment years. Values of proportion at the end of each year are presented in Supplementary Table D.2.

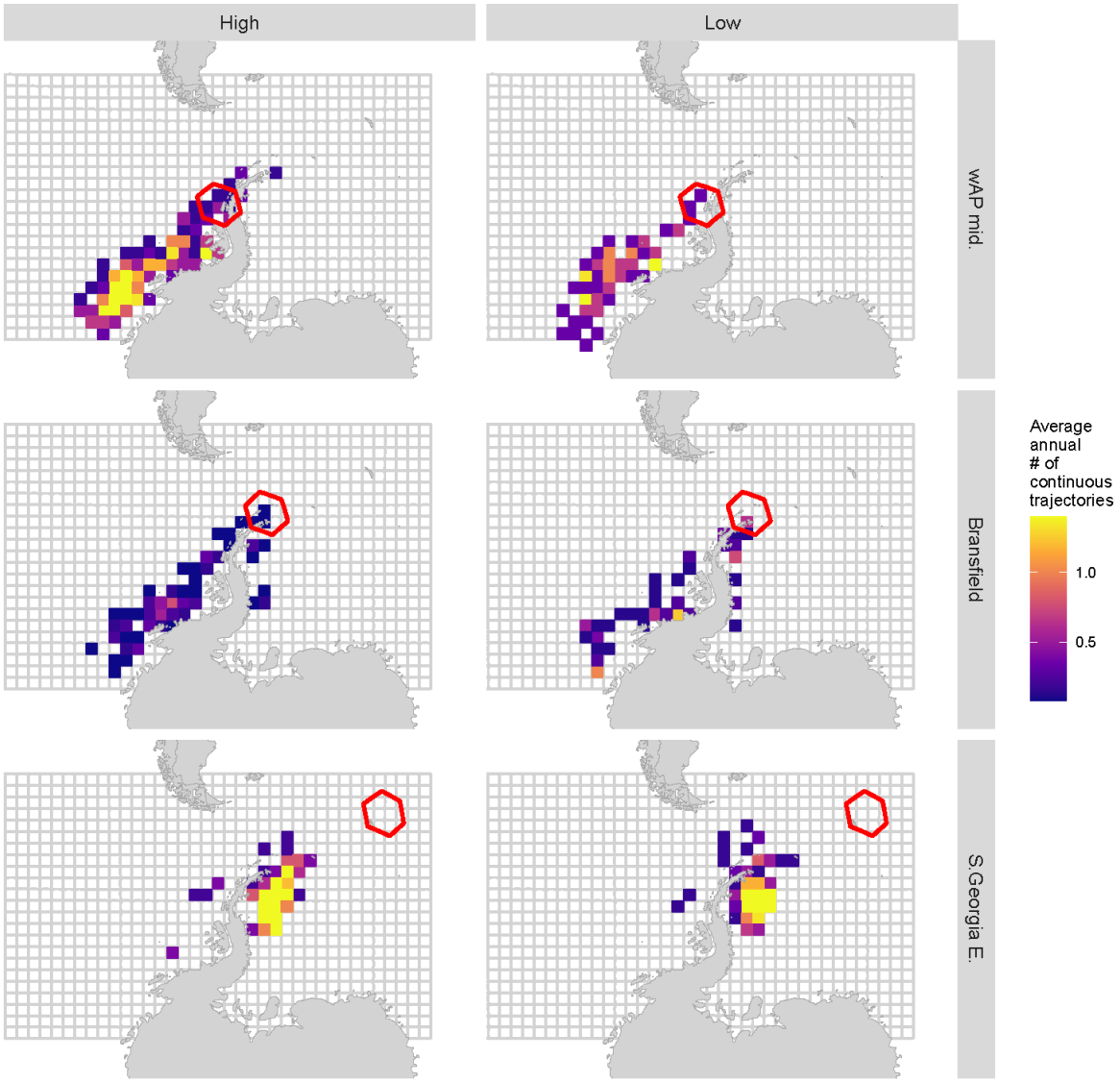

Figure D.7. The average annual number of continuous trajectories, binned to an equal-area 150 km by 150 km grid by location at the start of winter (*i.e.* the end of the back-trajectory on Julian day 90). Red hexagons indicate the recruitment region where the particles for the back-trajectories were seeded. To visualize the spatial patterns, binned counts were capped at the 90th percentile (maximum value = 7.2, 90th percentile = 1.4).

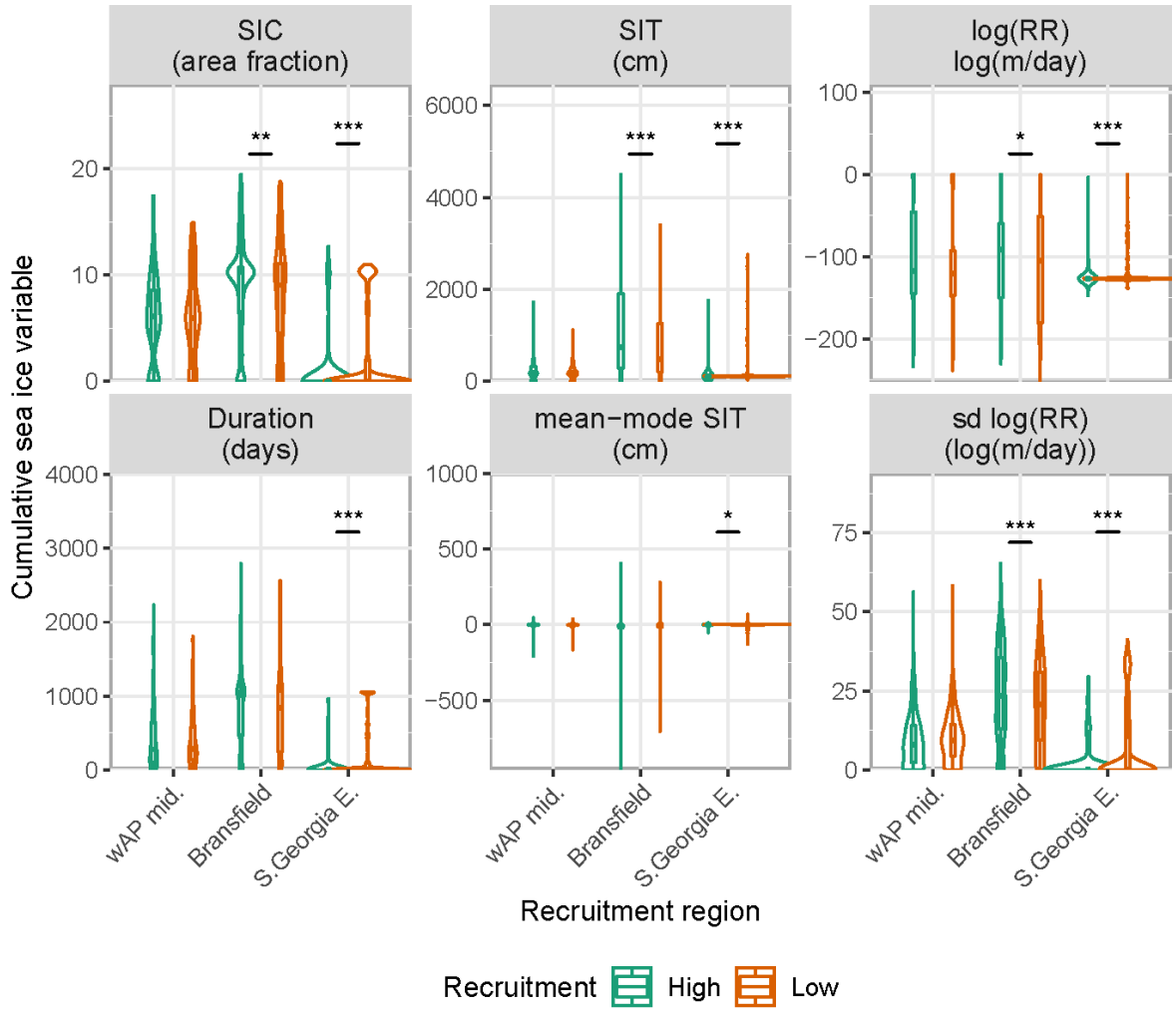

Figure D.8. The distributions of time-integrated habitat quality for fragmented trajectories. For each of the trajectories that were fragmented throughout the winter simulation, each sea-ice characteristic was integrated with respect to time. The distributions of these sums for each sea-ice characteristic are presented by recruitment region and recruitment success. Differences between the distributions in high and low recruitment years were tested using permutation tests (500 permutations for each test). Significant differences are indicated by the horizontal bars, with increasing numbers of asterisks indicating increasing confidence. Results from the permutation tests can be found in Supplementary Table D.4. Abbreviations used are as follows: sea-ice concentration (SIC), sea-ice thickness (SIT), ridging rate (RR) and standard deviation (sd).

Tables

Table D.1. The overall proportion of times each habitat driver contributes to habitat presence. This table therefore represents a proportion that comprises all the grid cells within each panel in Supplementary Fig. D.4.

Region	Recruitment classification	Proportion of both MIZ and SIT	Proportion of only MIZ	Proportion of only SIT
wAP mid	High	0.30	0.52	0.18
wAP mid	Low	0.08	0.76	0.15
Bransfield	High	0.18	0.66	0.16
Bransfield	Low	0.23	0.59	0.17
S.Georgia E.	High	0.22	0.68	0.10
S.Georgia E.	Low	0.21	0.72	0.07

Table D.2. The proportion of trajectories that remained continuous by the end of the simulation for each year. Note that the number of trajectories involved in each year's simulation (column 4) varies from year to year. This is due to short trajectories that run aground being cleaned from the analysis. Interannual differences in transport mean that this number will vary year to year. The p Proportion of continuous trajectories at end of winter represents column 5 divided by column 4.

Region	**Year**	**Recruitment Classification**	**Number of continuous trajectories at start of winter**	**Number of continuous trajectories at end of winter**	**Proportion of continuous trajectories at end of winter**
wAP mid	1981	High	132	70	0.53
wAP mid	1984	Low	131	30	0.23
wAP mid	1989	Low	138	58	0.42
wAP mid	2001	High	132	20	0.15
wAP mid	2008	Low	135	24	0.18
wAP mid	2010	High	139	12	0.09
wAP mid	2011	High	126	71	0.56
wAP mid	2012	High	130	105	0.81
wAP mid	2013	High	131	101	0.77
Bransfield	1980	Low	87	10	0.11
Bransfield	1981	High	73	11	0.15
Bransfield	1983	High	66	14	0.21
Bransfield	1984	Low	78	20	0.26
Bransfield	1987	High	70	32	0.46
Bransfield	1988	High	102	15	0.15
Bransfield	1989	Low	75	1	0.01
Bransfield	1991	High	68	18	0.26
Bransfield	1992	Low	68	12	0.18
Bransfield	1994	High	70	28	0.40
Bransfield	1995	High	84	17	0.20
Bransfield	1996	High	68	8	0.12
Bransfield	1997	High	92	24	0.26
Bransfield	1998	Low	62	7	0.11

Bransfield	2000	High	82	11	0.13
Bransfield	2001	High	86	17	0.20
Bransfield	2002	High	78	11	0.14
Bransfield	2003	Low	83	12	0.14
Bransfield	2004	Low	62	47	0.76
Bransfield	2005	Low	79	12	0.15
Bransfield	2006	High	64	9	0.14
S.Georgia E.	1981	High	86	37	0.43
S.Georgia E.	1983	Low	91	11	0.12
S.Georgia E.	1984	High	93	78	0.84
S.Georgia E.	1987	Low	93	43	0.46
S.Georgia E.	1995	High	91	39	0.43
S.Georgia E.	1996	High	91	39	0.43
S.Georgia E.	1997	Low	91	48	0.53
S.Georgia E.	2000	High	92	44	0.48
S.Georgia E.	2001	Low	81	59	0.73
S.Georgia E.	2003	Low	92	5	0.05
S.Georgia E.	2004	Low	98	26	0.27

Table D.3. Permutation test results: time-integrated habitat quality for continuous trajectories. Each permutation test compares the absolute difference between group means in high recruitment vs low recruitment years. Each test comprised 500 permutations. The permutation test result is the fraction of permutations where the permuted difference in absolute group means was less than observed. Each significant result was binned into a significance band. Abbreviations used are as follows: sea-ice concentration (SIC), sea-ice thickness (SIT), ridging rate (RR) and standard deviation (sd).

Region	**Sea-ice characteristic**	**Permutation test result**	**Significance band**
wAP mid	SIC	0	<0.001***
wAP mid	SIT	0	<0.001***
wAP mid	log(RR)	0.022	<0.05*
wAP mid	Duration	0	<0.001***
wAP mid	mean-mode SIT	0.59	
wAP mid	sd log(RR)	0.34	
Bransfield	SIC	0.064	
Bransfield	SIT	0.018	<0.05*
Bransfield	log(RR)	0.97	
Bransfield	Duration	0	<0.001***
Bransfield	mean-mode SIT	0.048	<0.05*
Bransfield	sd log(RR)	0.17	
S.Georgia E.	SIC	0.052	
S.Georgia E.	SIT	0.63	
S.Georgia E.	log(RR)	0	<0.001***
S.Georgia E.	Duration	0.76	
S.Georgia E.	mean-mode SIT	0.13	
S.Georgia E.	sd log(RR)	0.18	

Table D.4. Permutation test results: time-integrated habitat quality for fragmented trajectories. See table description for Supplementary Table D.3. Abbreviations used are as follows: sea-ice concentration (SIC), sea-ice thickness (SIT), ridging rate (RR) and standard deviation (sd).

Region	Sea-ice characteristic	Permutation test result	Significance band
wAP mid	SIC	0.75	
wAP mid	SIT	0.068	
wAP mid	log(RR)	0.064	
wAP mid	Duration	0.36	
wAP mid	mean-mode SIT	0.8	
wAP mid	sd log(RR)	0.22	
Bransfield	SIC	0.008	<0.01**
Bransfield	SIT	0	<0.001***
Bransfield	log(RR)	0.04	<0.05*
Bransfield	Duration	0.83	
Bransfield	mean-mode SIT	0.35	
Bransfield	sd log(RR)	0	<0.001***
S.Georgia E.	SIC	0	<0.001***
S.Georgia E.	SIT	0	<0.001***
S.Georgia E.	log(RR)	0	<0.001***
S.Georgia E.	Duration	0	<0.001***
S.Georgia E.	mean-mode SIT	0.022	<0.05*
S.Georgia E.	sd log(RR)	0	<0.001***

References

1 Veytia, D. *et al.* Overwinter sea-ice characteristics important for Antarctic krill recruitment in the southwest Atlantic. *Ecol. Indicators* **129**, 107934 (2021).

2 R Core Team. *R: A language and environment for statistical computing*, <https://www.R-project.org/> (2021).

3 Atkinson, A. *et al.* Krill (*Euphausia superba*) distribution contracts southward during rapid regional warming. *Nature Climate Change* **9**, 142-147, doi:10.1038/s41558-018-0370-z (2019).

4 Meyer, B. *et al.* The winter pack-ice zone provides a sheltered but food-poor habitat for larval Antarctic krill. *Nature ecology & evolution* **1**, 1853-1861 (2017).

5 Johnson, R., Strutton, P. G., Wright, S. W., McMinn, A. & Meiners, K. M. Three improved satellite chlorophyll algorithms for the Southern Ocean. *Journal of Geophysical Research: Oceans* **118**, 3694-3703 (2013).

6 Sumner, M. D. *raadtools: Tools for Synoptic Environmental Spatial Data. R package version 0.5.0.*, <https://github.com/AustralianAntarcticDivision/raadtools> (2018).

7 Quetin, L. *et al.* Growth of larval krill, Euphausia superba, in fall and winter west of the Antarctic Peninsula. *Mar. Biol.* **143**, 833-843 (2003).